CBCS SCHEME

USN | | | | | | | | | | |

18EE732

21EE742

Seventh Semester B.E. Degree Examination, Dec.2023/Jan.2024
Micro and Nano Scale Sensors and Transducers

Time: 3 hrs. Max. Marks: 100

Note: ***Answer any FIVE full questions, choosing ONE full question from each module.***

Module-1

1 a. Explain with neat diagram the working principle and structure of capacitive pressure sensors. **(08 Marks)**

b. Derive the expression for measuring pressure interms of inductance for inductive pressure sensor. **(08 Marks)**

c. Draw the block diagram of the interface circuit used to measure the capacitance 'C' of ultrahigh sensitivity pressure sensors. **(04 Marks)**

OR

2 a. Explain with neat diagram the working principle and structure of inductive pressure sensor. **(08 Marks)**

b. Derive the expression of pressure 'P' acting on the mercury drop as a function of capacitance in capacitive pressure sensor. **(08 Marks)**

c. Explain the graph of after – shock recovery time as a function of the applied pressure of ultra high sensitivity pressure sensors. **(04 Marks)**

Module-2

3 a. Explain with diagram the construction and working principle of acceleration sensor. **(08 Marks)**

b. Determine the gate voltage V_{GS} and ON – OFF operating points of the smoke detector. **(08 Marks)**

c. Analyze the following auxiliary experimental resultants of CO gas sensor.
i) Effect of temperature on the performance of sensor
ii) Effect of moisture on the performance of sensor. **(04 Marks)**

OR

4 a. Explain with neat diagram the working principle and structure of CO gas sensor. **(08 Marks)**

b. Derive the expression for measuring acceleration interms of capacitance of acceleration sensor. **(08 Marks)**

c. Analyze with graph the experimental of sensor output as a function of the distance between the α - particle source and the MOSFET gate of smoke detector. **(04 Marks)**

Module-3

5 a. Explain with neat diagram the operating principle of the advanced optical microphone. **(08 Marks)**

b. Develop the necessary mathematical relationship between the capacitance of the ultra-capacitor and conductivity of the electrolyte inside the moisture sensor. **(08 Marks)**

c. Explain with graph the probability of error as a function of the image size in optical micro-phone. **(04 Marks)**

OR

6 a. Explain with neat diagram the working principle and structure of moisture sensor. **(08 Marks)**

b. Explain with flowchart that shows how the code is structured and executed in optoelectronic microphone. **(08 Marks)**

c. Explain with graph the effect of contaminates like organic vapors and liquids on the performance of the moisture sensor. **(04 Marks)**

Module-4

7 a. Explain with neat diagram the principle operation of magnetic field sensor. **(08 Marks)**

b. Explain with necessary graphs the response of the magnetic field sensor to DC magnetic fields and to ac magnetic fields. **(12 Marks)**

OR

8 a. Explain with necessary diagram the general structure of "Lab on chip". **(08 Marks)**

b. Derive the expressions

i) Bending radius of the generated free electrons

ii) Deviation of the electrons path in the horizontal direction in magnetic field sensor. **(12 Marks)**

Module-5

9 a. Explain with diagram the principle of operation of the icing detector. **(08 Marks)**

b. Determine the turn ON condition and operating points of MOSFET used in icing detector. **(12 Marks)**

OR

10 a. Explain interface circuit diagram used in icing detector prototype. **(08 Marks)**

b. Analyze with proper graphs the following experimental results of icing detector.

i) Results of testing with dry air moist air, and super, saturated water vapor

ii) Results of testing with small crystal of ice

iii) Testing under lighting strikes **(12 Marks)**

* * * * *

Module - 1

1) a) Structure of capacitive pressure sensor –

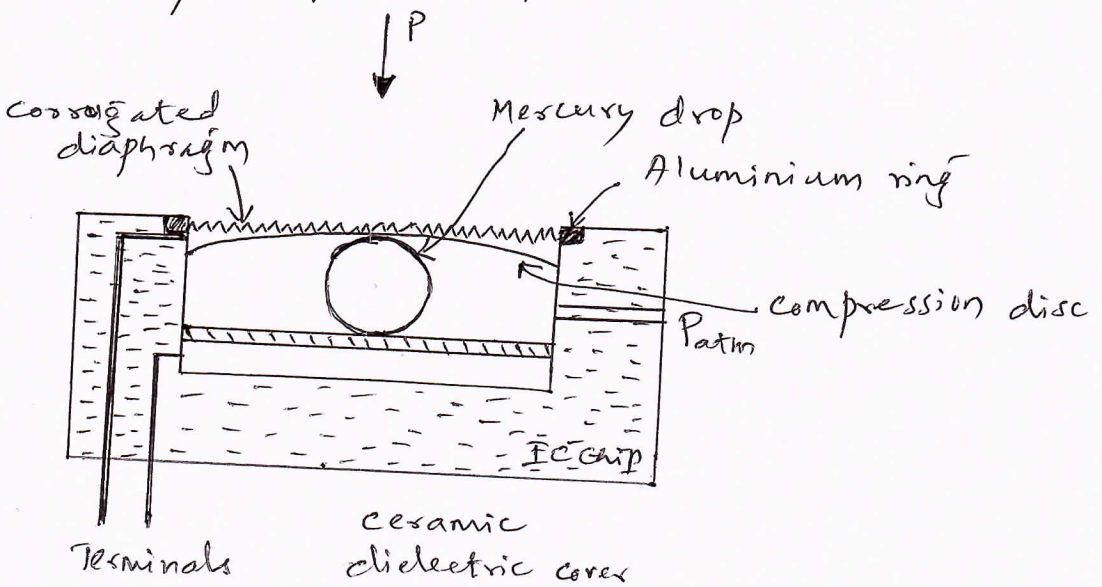

Working Principle :

In the basic structure of the sensor, a drop of mercury of 3 mm dia is placed on top of a flat aluminium electrode that is covered with a 1 μm thick layer of a ceramic material that has a very high dielectric constant. The drop is held in place by means of an aluminium disk that serves as the compression mechanism. The compression disk, in turn, is acted upon by means of a corrugated stainless steel diaphragm. The compression disk is given a slight curvature, such that the spacing between the disk & the ceramic layer is exactly 3 mm at the centre, but less than 3 mm everywhere else. In this manner, the mercury drop will be forced to the centre each time the stainless steel diaphragm retracts. The diaphragm is held in place by means of a thin aluminium ring. The entire assembly is mounted inside an open-cavity, 24-pin DIP IC package.

1) b) Expression for measuring pressure in terms of inductance for inductive pressure sensor –

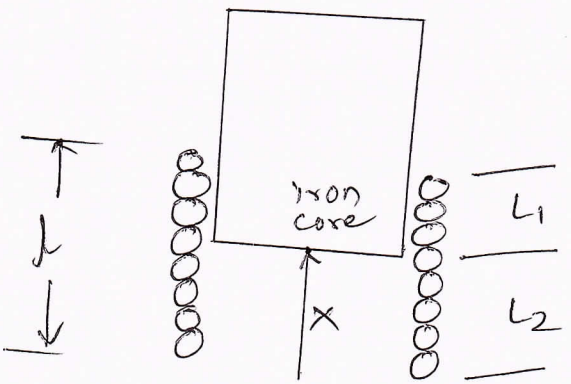

The inductive pressure sensor is based on a technique for substantially changing the inductance of a coil. The principle of this device is to create a highly variable inductance mechanism.

Inductance as a function of the position of the iron core :

The inductance L of any inductor is given by

$$L = \frac{\mu_0 \mu_r N^2 A}{l} \quad \text{——— (1)}$$

where, μ_0 → magnetic permeability of free space
μ_r → relative " present in the core
N → no of turns in the coil
A → c/s area of the coil
l → length

Based on the formula, inductances L_1 & L_2 will now be given in ~~the second inductor~~ terms of displacement x as follows:

$$L_1 = \frac{\mu_0 \mu_r N_1^2 A}{(l-x)} \quad \& \quad L_2 = \frac{\mu_0 N_2^2 A}{x} \quad \text{——— (2)}$$

where N_1 is the no of turns in the first inductor and N_2 is the no of turns in the second inductor.

The following relationships now must hold

$$N_1 + N_2 = N \quad \text{and} \qquad \text{——— (3)}$$

$$\frac{N_2}{N} = \frac{x}{l} \qquad \text{——— (3)}$$

$$\Rightarrow \quad \therefore N_1 = N\left(1 - \frac{x}{l}\right) \;\&\; N_2 = N\left(\frac{x}{l}\right) \qquad \text{——— (4)}$$

By substitution for N_1 & N_2. then

$$L_1 = \frac{\mu_0 \mu_r N^2 A}{l}\left(1 - \frac{x}{l}\right)$$

$$L_2 = \frac{\mu_0 N^2 A x}{l^2} \qquad \text{——— (5)}$$

$$\therefore \quad L = L_1 + L_2 = \frac{\mu_0 N^2 A}{l}\left[\mu_r - \frac{x}{l}(\mu_r - 1)\right] \qquad \text{——— (6)}$$

$$= L_0\left[\mu_r - \frac{x}{l}(\mu_r - 1)\right]$$

The min. pressure P_{min} that must be applied to the sensor is

$$P_{min} = \frac{F_{min}}{A}$$

where $F = k \cdot x = (P - P_{min})A \qquad \text{——— (7)}$

where k is the spring constant & P is the pressure acting on the sensor.

Hence the displacement x of the iron core is.

$$x = \frac{(P - P_{min})A}{k} \qquad \text{——— (8)}$$

Applied pressure as a fn of the observed inductance, 'L' is,

$$L = L_0 \left[\mu_r - (\mu_r - 1) \left(\frac{(P - P_{min})A}{kl} \right) \right] \quad \text{— (9)}$$

solving for P,

$$P = P_{min} + \frac{kl}{A} \left(\frac{\mu_r - L/L_0}{\mu_r - 1} \right) \quad \text{— (10)}$$

---

1) c) Interface circuit used to measure the capacitance 'C' of ultrahigh sensitivity pressure sensor-

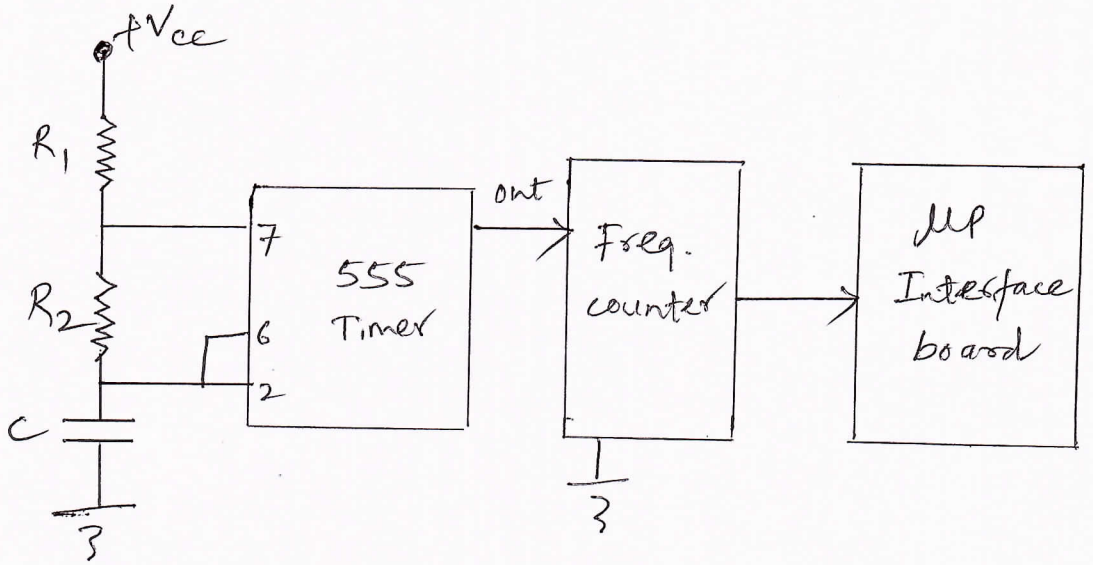

The interface circuit is a well-known 555 oscillator circuit that converts an unknown capacitance to freq. The interface ckt. does not amplify or compensate for the characteristics of the sensor.

2/a) Inductive Pressure Sensor -

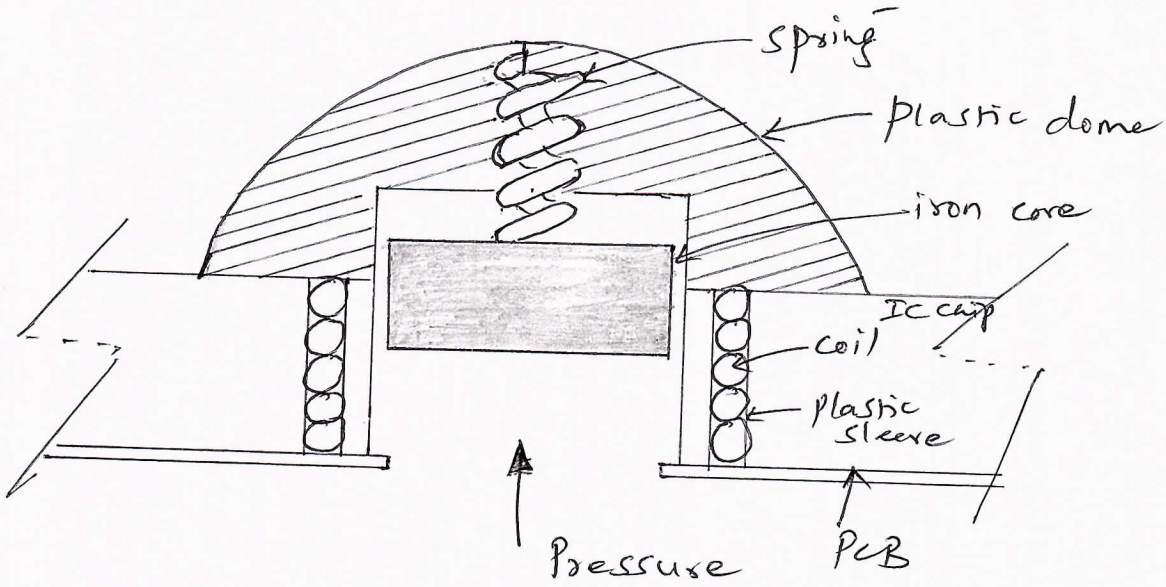

Structure & working principle -

The principle of inductive pressure sensor is to create a highly variable inductance mechanism. In the mechanism shown, the change in inductance is equal to the relative magnetic permeability of the core material and is typically 4000-fold or higher.

As shown in the figure, a vertical coil of a height & diameter is totally embedded inside an open cavity, 24-pin DIP package. A small cylindrical iron core is positioned inside the coil, surrounded by a smooth Teflon sleeve.

The pressure acts on the iron core in the upward direction. A semi-spherical plastic dome is positioned on top of the coil in order to contain the iron core it displaced. In the internal cavity of the dome, a spring with a known spring constant is mounted. As the displaced iron core exerts force on the spring, the displacement will be proportional to the force that is acting on the iron core.

5

2) b)

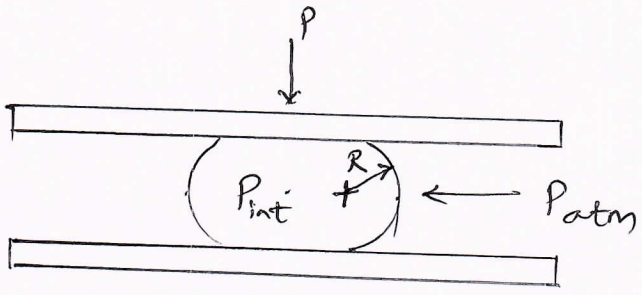

The above fig. shows the geometry of a drop of mercury that is deformed between two solid surfaces. The vertical pressure that is acting on the drop is 'P', and the lateral pressure is atmospheric pressure P_{atm}. P_{int} is the internal pressure and 'R' is the radius of curvature of the part of the surface of the liquid that is not flattened.

The internal pressure P_{int} in the liquid must be balanced by the atmospheric pressure plus the Laplace pressure, or the pressure due to surface tension ie,

$$P_{int} = P_{atm} + \frac{2\gamma}{R} \quad \text{——} (1)$$

where $2\gamma/R$ → Laplace pressure

γ → surface tension of the mercury

As the drop of mercury is flattened then,

$$P = P_{int} - (P_{int})_0 \quad \text{——} (2)$$

where $(P_{int})_0$ → internal pressure at zero applied pressure.

∴ From eqns (1) & (2) ⇒

$$P = P_{atm} + \frac{2\gamma}{R} - \left(P_{atm} + \frac{2\gamma}{R_0}\right) \quad \text{——} (3)$$

where R_0 is the original unflattened radius of the drop. Hence,

$$P = 2\gamma\left(\frac{1}{R} - \frac{1}{R_0}\right) \quad \text{——} (4)$$

The capacitance of parallel plate capacitor is given by

$$C = \frac{\epsilon A}{d} \quad \text{——— (5)}$$

For the wetting area 'A' of the deformed drop,

$$A = \pi \left[\sqrt{\frac{\pi^2 R^2}{16} + \frac{2R_0^3}{3R}} - \frac{\pi}{4} R \right]^2 \quad \text{——— (6)}$$

& $$R = \sqrt{\frac{Cd}{\epsilon \pi^3} + \frac{4}{3} R_0^3 \left(\frac{\epsilon}{\pi C d}\right)^{1/2}} - \sqrt{\frac{Cd}{\epsilon \pi^3}} \quad \text{——— (7)}$$

From eqns (6) & (7) ⇒

Pressure 'P' acting on the mercury drop can be formulated as a fn of capacitance 'C', i;

$$P = 2\gamma \Big/ \left(\sqrt{\frac{Cd}{\epsilon \pi^3} + \frac{4}{3} R_0^3 \left(\frac{\epsilon}{\pi C d}\right)^{1/2}} - \sqrt{\frac{Cd}{\epsilon \pi^3}} \right) - \frac{2\gamma}{R_0} \quad \text{——— (8)}$$

2/c)

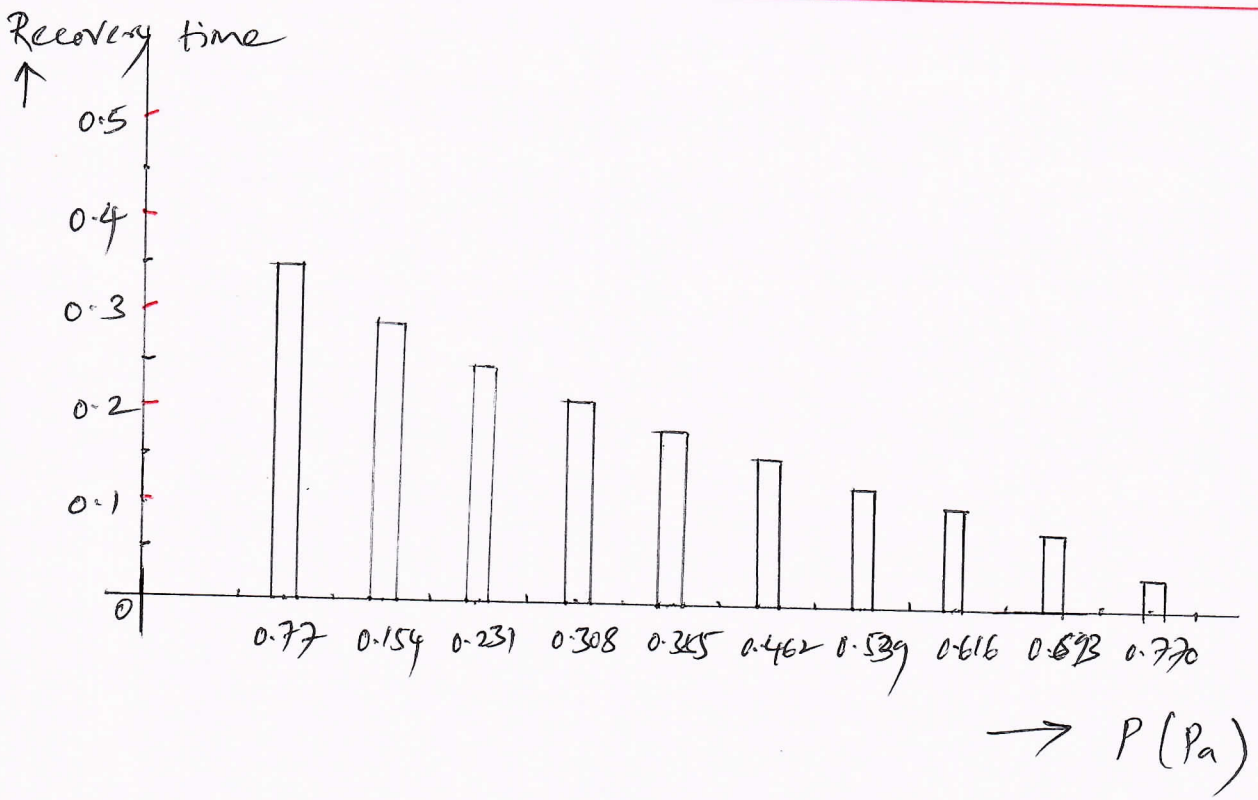

If the sensor is shocked, the moving electrode will be momentarily displaced, and it was observed that a "recovery time" is needed for the moving electrode to return to its original position.

In order to determine the recovery time that is needed for the error to disappear after the shock, ~~pulses of a magni~~ the freq. of an interface circuit uses a 555 oscillator was monitored with a digital storage oscilloscope. The normal freq. of the interface circuit was noted and the time duration that lapsed from the onset of the shock until the freq. returned to its normal value was observed on the scope. The results of the test are shown in the above graph.

Module - 2

5) a) Construction & Working Principle of acceleration Sensor –

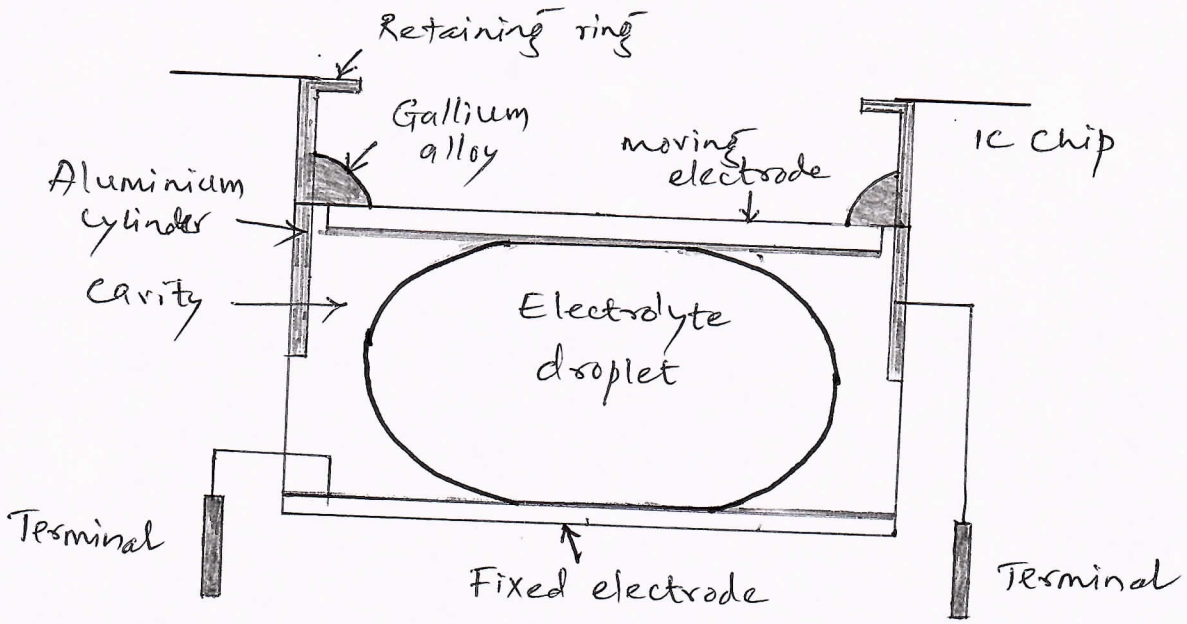

As shown in the figure, the electrolyte droplet the fixed electrode, and the moving electrode are placed inside the cavity in the SOIC chip. A very Thin aluminium cylinder with a height of approximately one half of the cavity is also inserted in the cavity. The purpose of the cylinder is to act as a contact terminal for the moving electrode. A small piece of conductive metal known as "Liquid Metal" is placed on top of the moving electrode and serves to establish electrical contact b/w the electrode & the aluminium cylinder. A steel ring is placed on top of the cavity and serves to retain the moving electrode and hence the electrolyte droplet, inside the cavity.

3) b) Determination of the gate voltage, V_{GS} :

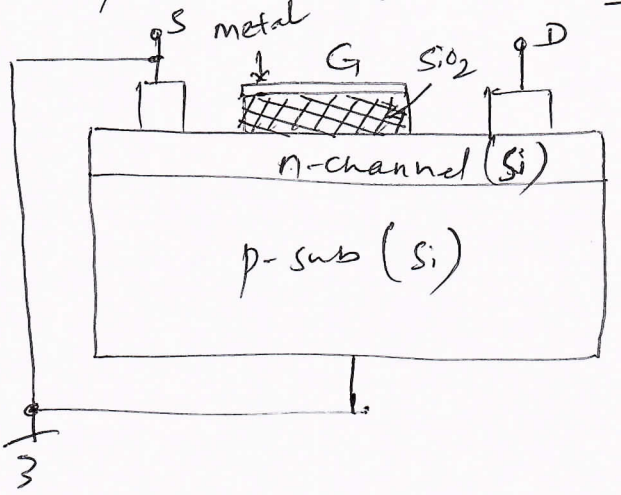

The steady-state current that will be flowing in to the gate terminal will be given by

$$I = \frac{dQ}{dt} = \frac{7400 \times 1.6 \times 10^{-19}}{1} = 1.18 \times 10^{-15} \text{ A} \quad \text{—— (1)}$$

The leakage current density 'J' thro' the SiO_2 is related to the electric field intensity 'E' b/w G & S terminals is.

$$J = \sigma E \quad \text{—— (2)}$$

where σ is the conductivity of SiO_2

$$\therefore \frac{I}{A} = \sigma \frac{V_{GS}}{\Delta x} \quad \text{—— (3)}$$

$$\therefore V_{GS} = \frac{I \Delta x}{\sigma A} \quad \text{—— (4)}$$

but $$C = \epsilon_0 \epsilon_r \frac{A}{\Delta x} \quad \text{—— (5)}$$

where ϵ_0 is the permittivity of the free space & ϵ_r is the relative permittivity of SiO_2

$\therefore$ The ratio, $\frac{\Delta x}{A} = \frac{\epsilon_0 \epsilon_r}{C}$ by 1.438 m^{-1} —— (6)

$\therefore$ The steady state V_{GS} approximately found to be 17V after

Determination of the ON-OFF operating points of the smoke detector –

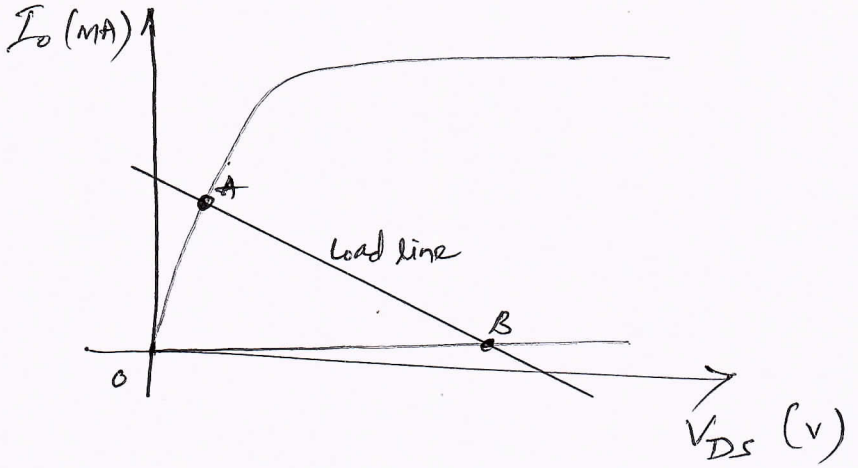

The above fig. shows the load line. ~~for~~
When $V_{GS} = 0$, the MOSFET will be cut-off & $V_{DS} \simeq V_{cc}$.
To determine the upper operating point, the following two eqns must be solved:

$$I_D = \frac{V_{cc}}{R} - \frac{1}{R} V_{DS} \qquad \text{——— (1)}$$

$$I_D = \frac{V_{DS}}{R_{on}}$$

where, $R \rightarrow$ value of load resistance
$R_{on} \rightarrow$ ON resistance of the MOSFET.

$$\therefore V_{DS} = \frac{V_{cc}}{1 + \frac{R}{R_{on}}} \qquad \text{——— (2)}$$

3) c) i) Effect of temperature on the performance of the sensor –

The reaction rate (hence the sensor's response) is quite acceptable at room temp., but can be much more worse at substantially lower temperatures. The sensor was also tested at elevated temperatures (up to 80°c), and the reaction rate was found to be generally higher at such temperatures.

ii) Effect of moisture on the performance of the sensor –

Moisture was added to the gas/air mixture, and the relative humidity in the mixture was monitored with a moisture sensor.

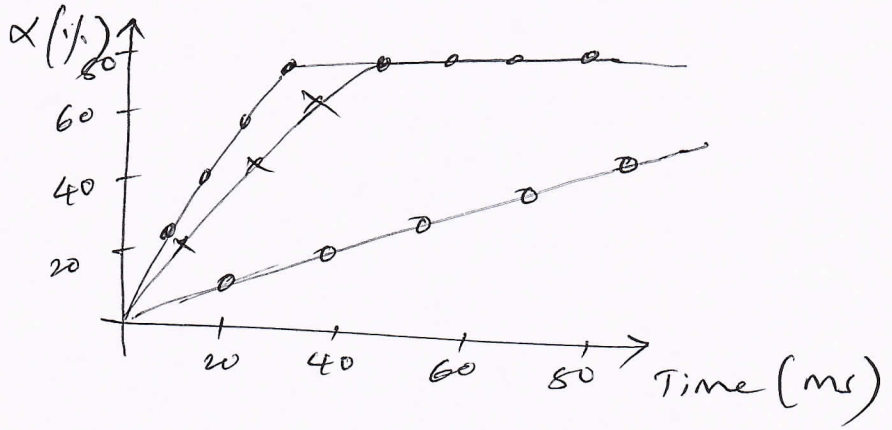

The above graph shows the result of a test that was conducted at room temp. & with a CO concentration of 100 ppm. As the fig. shows, the effect of moisture was negligible for the relative humidity range of 5% to 40%. For the range of RH from 40% to 80%, however, the reaction rate slowed significantly. This can be understood on the basis of the fact that sensor assembly will be less in this case.

4) a) CO gas sensor -

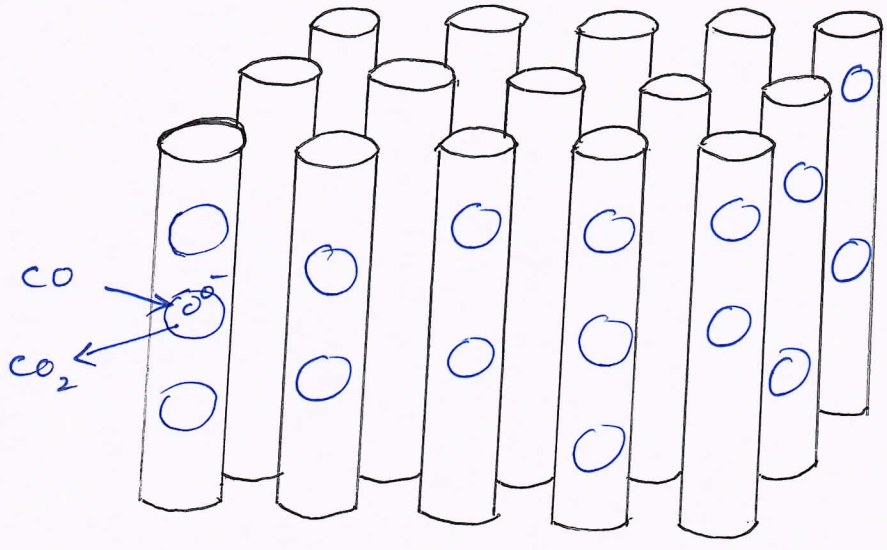

Structure -

As shown in the figure, gold nanoparticles are attached to an array of multiwalled carbon nanotubes. Gold nano particles have a large affinity for oxygen and oxygen molecules become absorbed on the large surface presented by the nano particles, where they easily dissociate. CO, a reducing gas, easily combines with atomic oxygen & releases free electrons according to a well known reaction. The presence of extra free electrons reduces the overall resistivity of the carbon nano tube array, which can be detected with an external circuit.

The two reactions that can be synthesized with catalyst are,

$$2CO + O_2^- \rightarrow 2CO_2 + e^- \qquad \text{—— (1)}$$

$$CO + O^- \rightarrow CO_2 + e^-$$

According to the principle, these well known chemical reactions are synthesized in the new solid-state detector by using the excellent catalytic activity of gold nano-particles.

The miniature solid-state CO detector described has the following characteristic advantages:

- Sensitivity to CO concentrations of less than 100 ppm at room temp.
- Can be battery operated, with a very long battery life
- Being a miniature detector, it can be placed virtually anywhere.

Working Principle-

The rate of the catalytic reactions can be described by the well-known reaction rate eqn

$$-\frac{dp}{dt} = k_0 \cdot \exp\left(-\frac{E_a}{RT}\right) p^m \quad \text{——— (2)}$$

where $P \rightarrow$ partical gas pressure
$k_0 \rightarrow$ pre-exponential factor
$E_a \rightarrow$ activation energy
$m \rightarrow$ pseudo-kinetic order of the reaction of CO by various catalysts.

$$\alpha(t) = k_0 \cdot \exp\ 1 - \frac{P(t)}{P_0} \quad \text{——— (3)}$$

where P_0 is the partial pressure of CO at $t=0$.

If $m=1$ then eqn (2) becomes

$$P = P_0 \exp\left(-k_0 \exp\left(-\frac{E_a}{RT}\right)t\right), \quad m=1 \quad \text{——— (4)}$$

$$\therefore \alpha = 1 - \exp\left(-k_0 \exp\left(-\frac{E_a}{RT}\right)t\right), \quad m=1 \quad \text{——— (5)}$$

If $m=0$ then, $P = P_0 - k_0 \exp\left(-\frac{E_a}{RT}\right)t, \quad m=0$ ——— (6)

$$\therefore \alpha = \frac{k_0}{P_0} \exp\left(-\frac{E_a}{RT}\right)t, \quad m=0 \quad \text{——— (7)}$$

4) b)

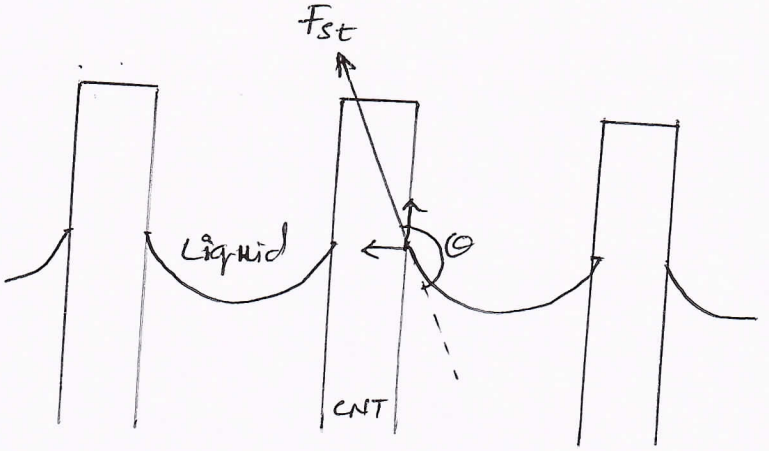

An array of CNT's that is penetrating a liquid electrolyte and for each CNT hydrophobic force will be given by

$$F = 2\pi r \gamma \cos(180^\circ - \theta) \quad \text{——— (1)}$$

where r → radius of one CNT
γ → surface tension of the fluid
θ → liquid-solid contact angle.

The total upward force that is acting on the fluid will be given by NF, where N is the total no. of CNT's penetrating the fluid.

Given an electrode with a mass m that is moving with a uniform acceleration a, the Newtonian force $F = ma$ must be balanced by the total hydrophobic force, ie,

$$F_{total} = ma = 2\pi r N \gamma \cos(180^\circ - \theta) \quad \text{— (2)}$$

The surface area A of the CNT's that is immersed in the electrolyte will be given by,

$$A = 2\pi r \sum_{i=1}^{N} x_i \quad \text{——— (3)}$$

where x_i is the immersion depth of any given CNT.
The capacitance of the electrode-electrolyte interface is now given by,

$$C = \frac{\epsilon_0 \epsilon_r A}{d} \quad \text{——— (4)}$$

By taking $\epsilon_r \approx 1$, we have

$$C = \frac{\epsilon_0}{d}\left(2\pi r \sum_{i=1}^{N} x_i\right) \quad \text{——— (5)}$$

From eqn (5), the series combination of C_1 & C_2 can be expressed as,

$$C_{total} = K\,\frac{\epsilon_0}{d}\left(2\pi r \sum_{i=1}^{N} x_i\right) \quad \text{— (6)}$$

where 'k' is the constant ranges from 1 to 0.5

$$\therefore \quad Ma = N\gamma \cos(180^\circ - \theta)\left(\frac{dC_{total}}{K\epsilon_0 \sum_{i=1}^{N} x_i}\right) \quad (7)$$

Hence,

$$a = -\frac{dN\gamma\cos\theta}{KM\epsilon_0 \sum_{i=1}^{N} x_i} \quad \text{——— (8)}$$

$$a = -\frac{d\gamma\cos\theta}{KM\epsilon_0 x} \cdot C_{total}, \quad \theta > 90^\circ$$

---

4) c)

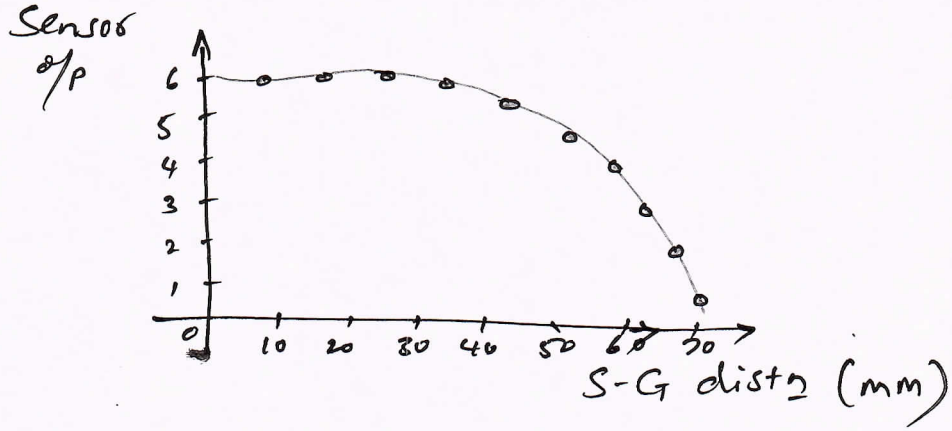

The o/p of the sensor was measured as a fn of the distance between the α-particle source & the gate of the MOSFET.

The MOSFET is known to be slightly sensitive to temp. And the drain current I_D decreases at temperatures higher than room temp. & increases at lower temp.

Module-3

5) a) **Optical microphone** -

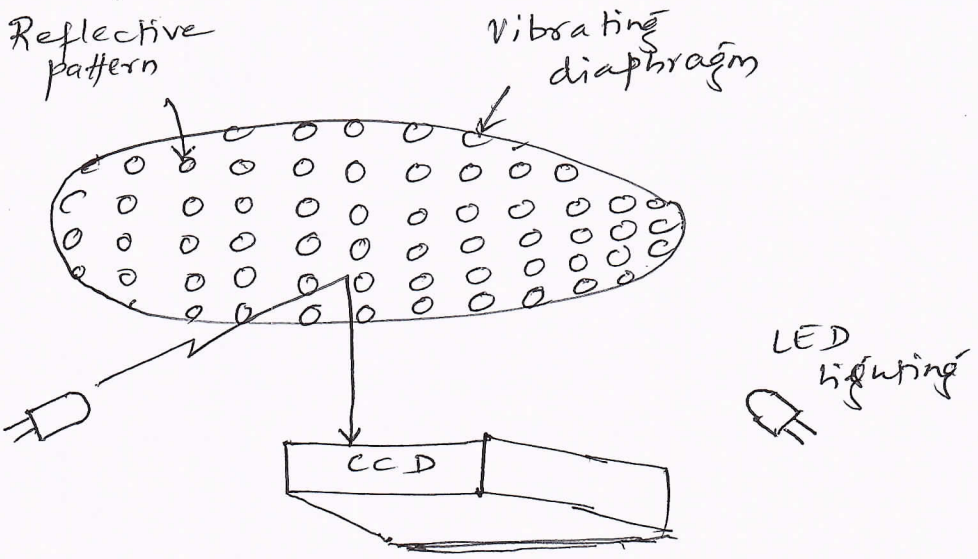

As shown in the above fig., a conventional, thin metallic diaphragm vibrates in response to sound pressure. The diaphragm has a reflective pattern that is etched on its surface. A group of LED's are arranged underneath the diaphragm to illuminate the reflective pattern. The image of the pattern is then captured by a CCD & is passed to a microprocessor for pattern recognition. Hence, the pattern recognition is the distinctive new feature in this type of microphone.

---

5) b) **Mathematical relationship between the capacitance of the ultra capacitor & conductivity of the electrolyte inside the moisture sensor** –

current density, $J = \sigma E$ —— (1)

J & E are further related to the current I & V by $J = \frac{I}{A}$ and $E = \frac{V}{d}$ —— (2)

$\therefore \frac{I}{A} = \sigma \frac{V}{d}$ —— (3)

The current thro' the electrolyte will be related to the rate of flow of charges by

$$I = \frac{dQ}{dt} \quad \text{—— (4)}$$

$$\therefore \frac{dQ}{dt} = \frac{AV}{d}(\sigma(t)) \quad \text{—— (5)}$$

Here, the conductivity is assumed to be a time-varying quantity and the v.g. 'V' across the terminals of the ultra capacitor is assumed to be constant.

Hence, $$Q = \frac{AV}{d}\int \sigma(t)\, dt \quad \text{—— (6)}$$

$$\therefore Q = C_{int} V_{int} \quad \text{—— (7)}$$

where C_{int} → capacitance of the interface
V_{int} → v.g. across the interface.

From eqns (6) & (7) $\Rightarrow \frac{1}{2} C_{int} V = \frac{AV}{d}\int \sigma(t)\, dt$ —— (8)

or $$C_{int} = \frac{2A}{d}\int \sigma(t)\, dt \quad \text{—— (9)}$$

$$\therefore C = \frac{A}{d}\int \sigma(t)\, dt$$

---

5) c)

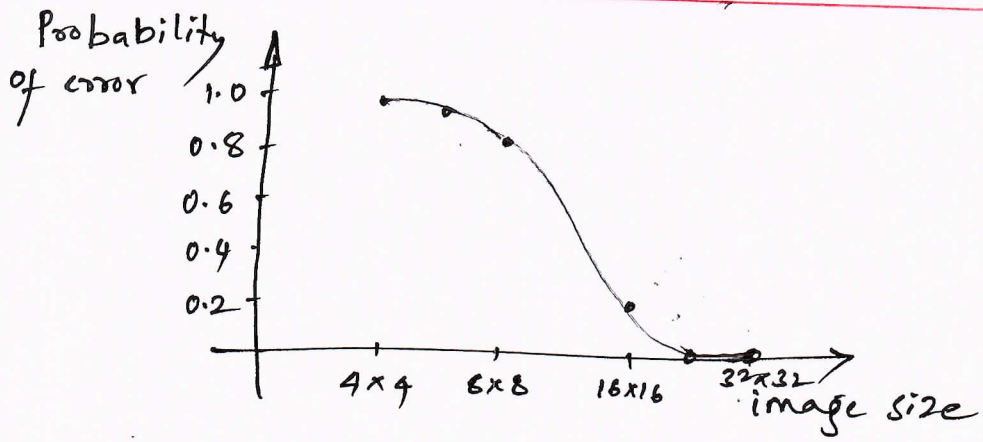

Probability of error as a function of image size

The probability of calculating the displacement $x(t)$ incorrectly was measured as a fn of the image size. The above graph shows the results at 20 db SPL. All the measurements were performed inside an anechoic chamber. The microphone was subjected to a sinusoidal sound pressure wave and a Bruel & Kjaer Model 2236 sound pressure meter was used as a reference for determining the acoustic pressure. Clearly, the probability of error increases substantially as the size of the image matrix becomes smaller.

6) a) Moisture sensor -

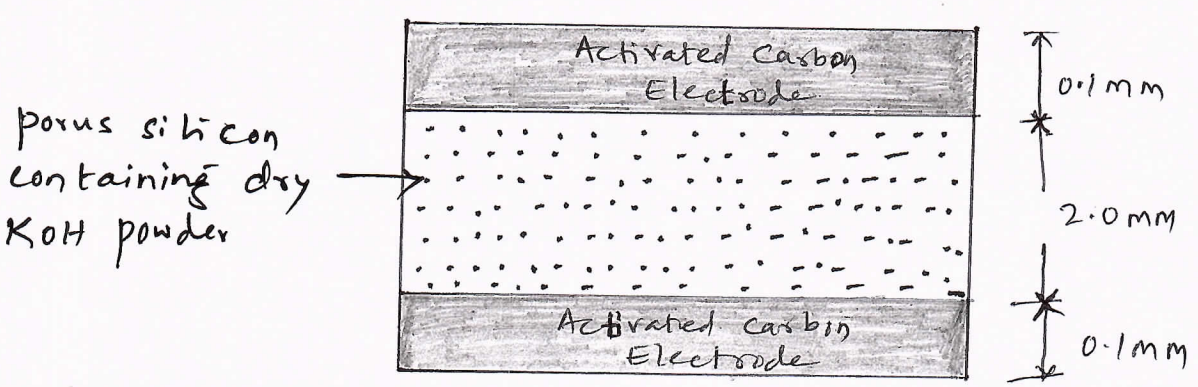

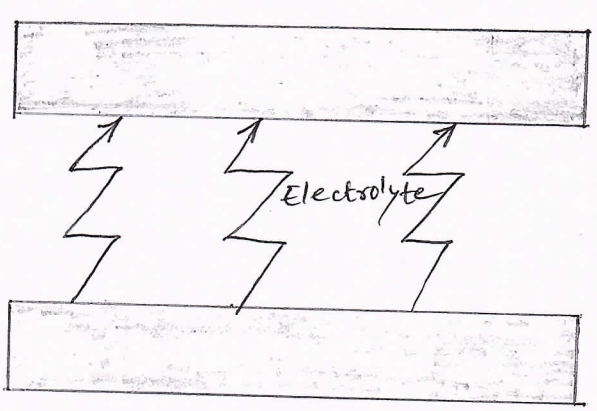

Structure :

The moisture sensor is based on the idea of using an ultracapacitor structure rather than an ordinary capacitor. Inside the ultracapacitor, the moisture itself constitutes the electrolyte that is

needed for charge transfer.
This sensor has the highest sensitivity w.r.t. size among all known types of moisture sensors. Such sensors will therefore be very useful in applications such as the detection of moisture in small electronic packages & components detection of moisture inside composite ~~aircraft~~ aircraft materials, and other embedded moisture sensing applications.

The porous silicon slab was obtained from a commercial supplier of porous silicon. The mean pore size of the pores in the slab is approximately 10 nm. To embed the KOH powder inside the slab, KOH at a concentration of 35% by weight was first dissolved in distilled water, and the slab was soaked in the solution. The slab was then sintered in a furnace at a temp. of 500°C for 30 min. to remove the water. The activated carbon electrodes were subsequently deposited on both sides of the slab.

---

6) b) Flow chart for showing how the code is structured & executed in optoelectronic microphone –

As per the flow chart shown, the last step in the code is the equilization step. Equilization is performed to obtain a flat freq. response and is a common procedure in digital microphones.

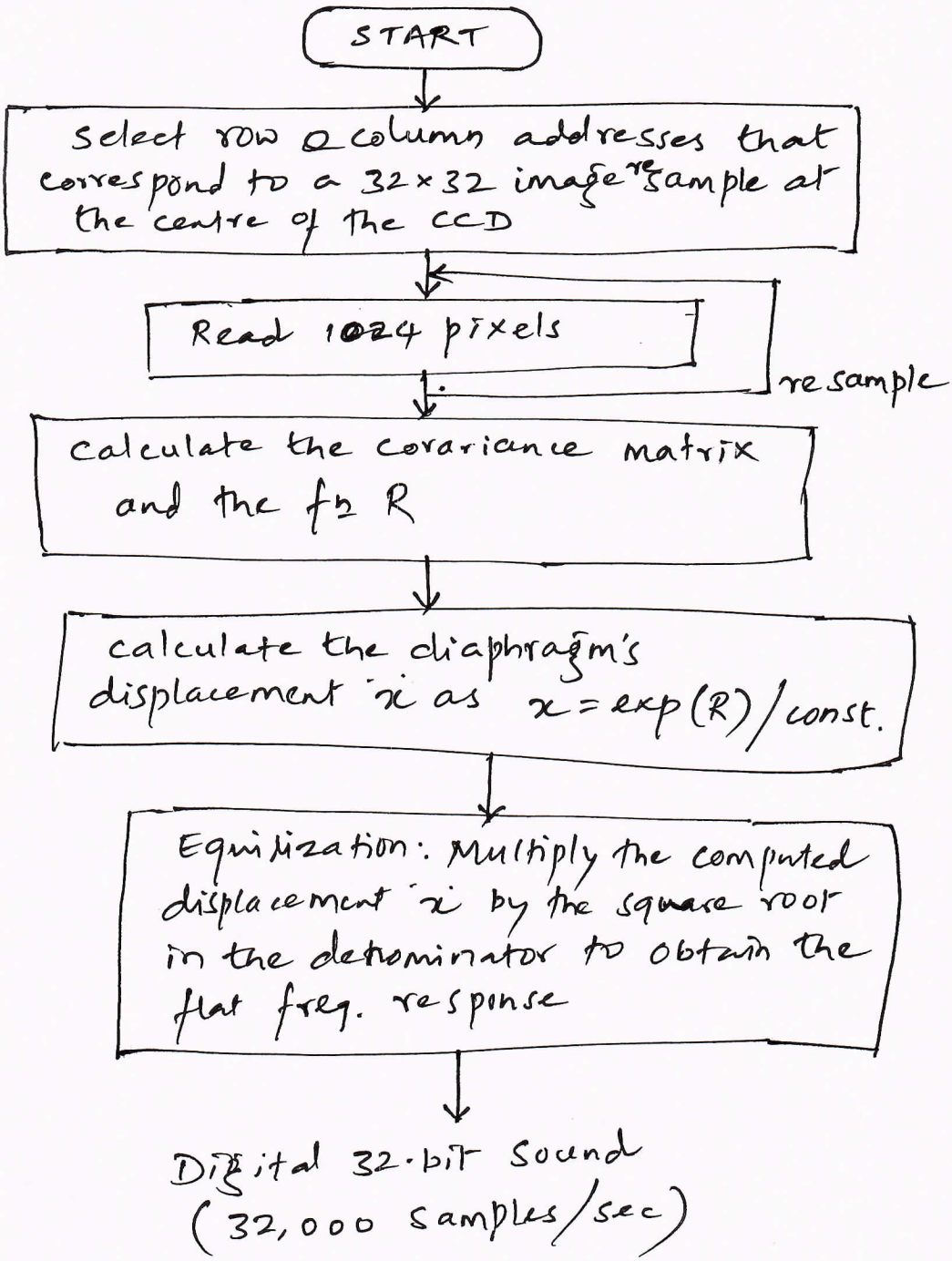

6) c) Effect of contaminants like organic vapors & liquids on the performance of the sensor -

To test the effect, a s/m was devised in which the sensor was placed in a small vacuum chamber that is connected to a computer-controlled evaporator. The evaporator, in turn, is connected to a cylinder that supplies dry N_2 gas. The N_2 gas is circulated thro' the chamber & mixed with the vapors emerging from the evaporator. The control system maintains precise control of the concentration

of the contaminant vapor within the N_2 gas.
Three solvents were tested: benzene, ethanol, & water.

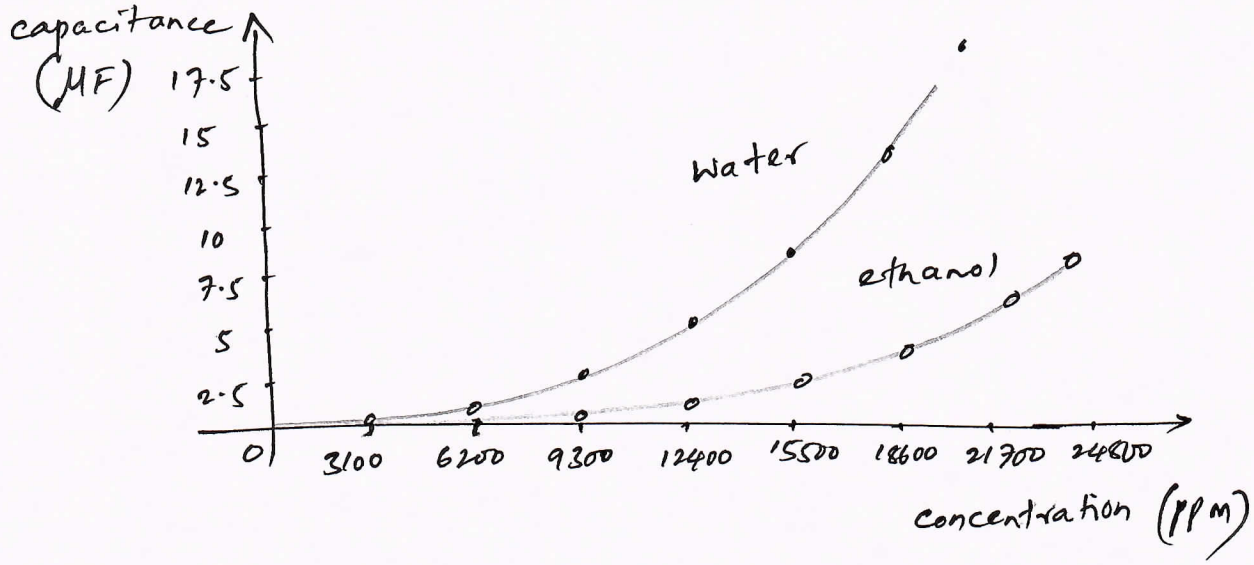

The above graph ~~solve~~ shows the results, where the measured capacitance of the sensor is plotted against the concentration of the vapor in ppm.

The conclusion is that, the presence of organic contaminants will degrade the performance of the sensor. Of course, the degradation will depend on the ratio of the contaminant to the water present in the moisture.

Module - 4

7) a) **Magnetic Field Sensor :**

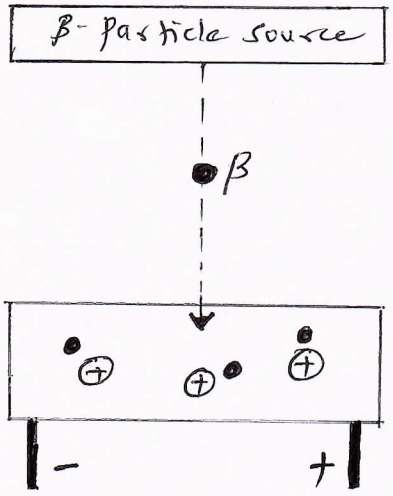

Fig (a)

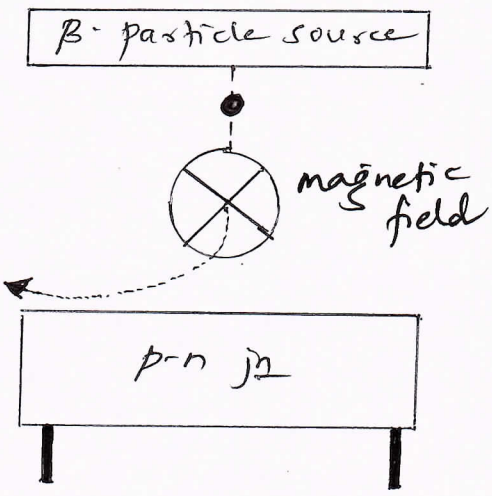

Fig (b)

Principle of operation -

The magnetic field sensor depends on the beta-Voltaic principle. Fig (a) shows, a source of low energy β particles is positioned above a p-n jn. As the β-particles enter the p-n jn, a electron-hole pairs are produced inside the jn and a vg. appears a/c the terminals of the jn.

In Fig (b), a magnetic field is applied in a direction that is perpendicular to the direction of motion of the β-particles. As a result, the β-particles follow a curved path and miss the p-n jn, and the voltage across the terminals of the jn therefore drops in magnitude. Such drop in vg. is related to the intensity of the applied magnetic field by a formula

7b) Response of the sensor to DC magnetic fields -

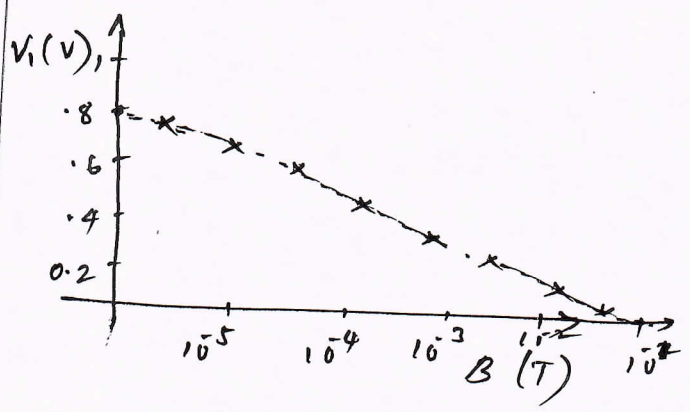

(a)

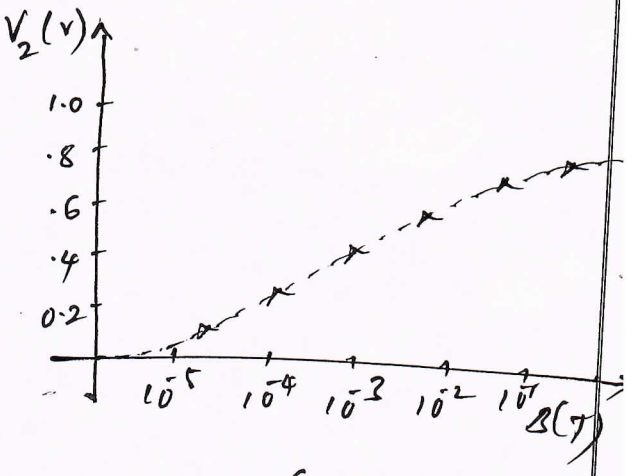

(b)

A magnetic flux, with a density B ranging from 10^{-6} T to 0.1 T was applied to the sensor. The magnetic field was generated with a simple, custom-made electro magnet that was placed in the vicinity of the sensor. Once again, the magnetic field of the earth was shielded by placing the experimental set up inside a nickel-iron enclosure. The graphs (a) & (b) shows the measured voltages V_1 & V_2 across the inner & outer p-n jns. resply, as the field was increased from 10^{-6} T to 0.1 T.

From the graphs, it is of course apparent that the vg. will be a non-linear fn of the applied magnetic flux density. In practical applications, the magnetic flux density can be inferred from the measured vg. V_1 or V_2, by inspection of the corresponding curve as shown.

Response to Ac magnetic fields -

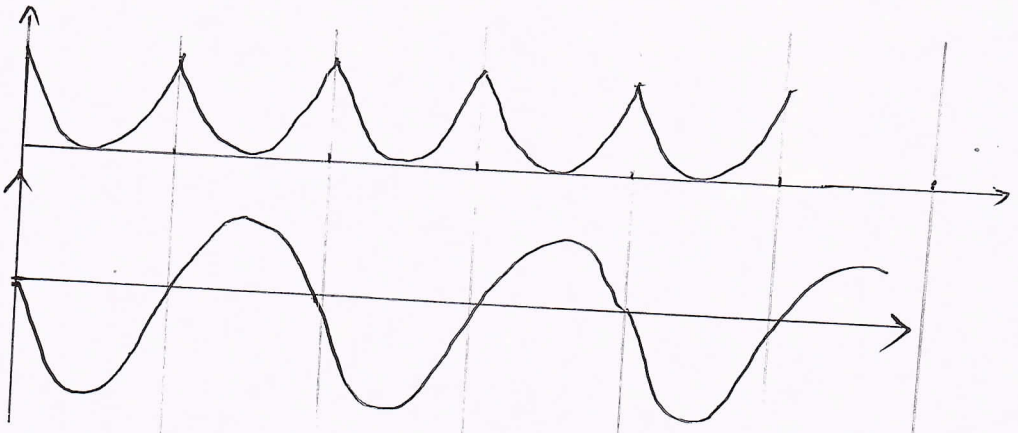

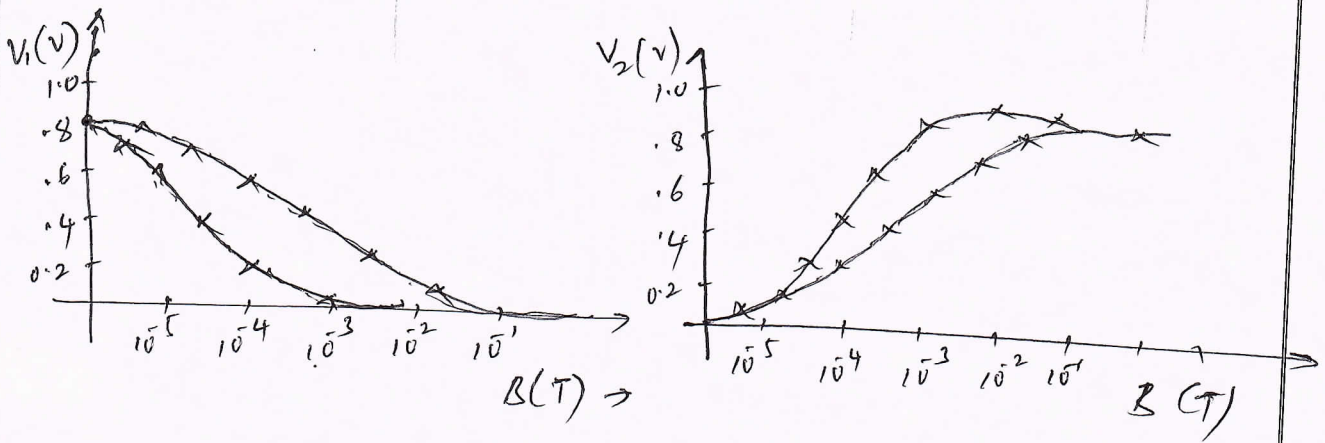

The above graph shows the response of the sensor to an alternating field with a peak value of 0.1T and a freq. of 600 Hz. The low freq. was choosen for better visulization.

The response form the graph can be understood as follows: as the magnetic flux density increases in value, the EHP current thro' the inner p-n jn is "chocked off" until it reaches '0' at the point of max. applied field (0.1T). The vg. across the inner jn increases again to 0.8 V as the field weakens and, as the field reserves polarity, the EHP current decreases once again & the same cycle is repeated.

8) a) Lab on Chip -

General structure -

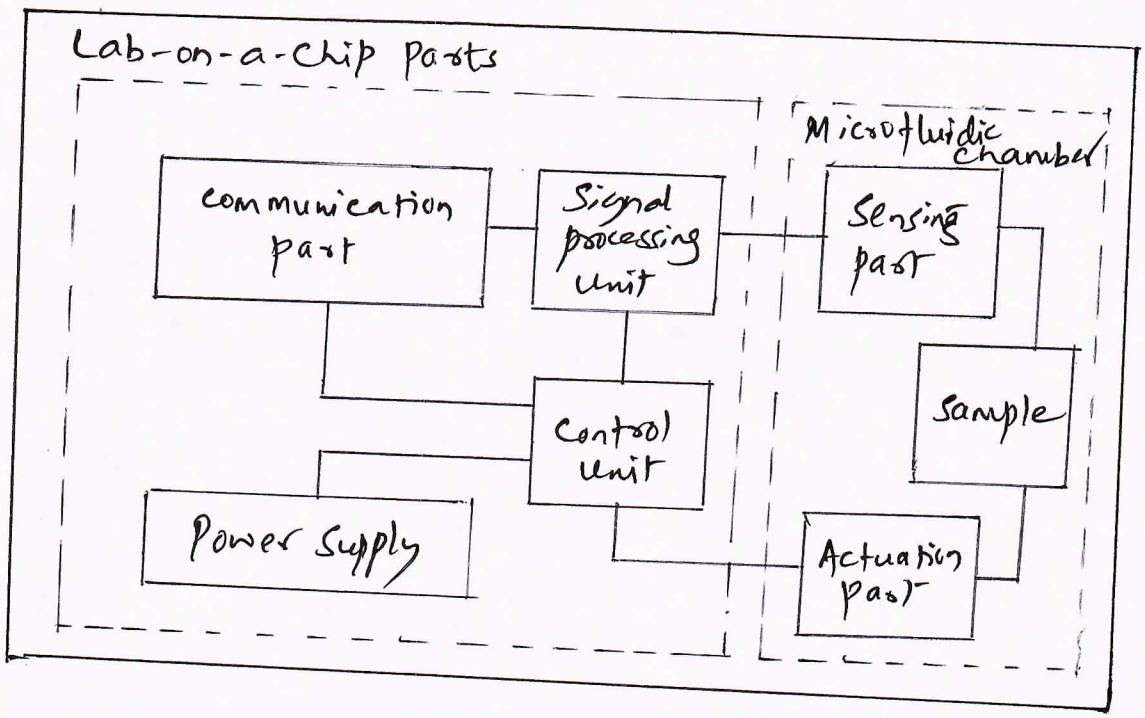

As shown in the figure, Lab-on-a-Chip essentially composed of three sections : actuation, sensing, & electronic interface circuitry.

The Lab-on-chip solutions that currently exist can easily perform diagnostic operations such as microorganism detection & characterization, flow cytometry applications, polymerase chain reaction (PCR), in addition to many others.

In the actuation section, the chip generates electrical or mechanical forces that act on the biological sample. In the sensing section, sensors that are embedded in the chip measures responses that may be electrical, optical, thermal, or magnetic, and route the detected signals to the electronic section for final processing. The electronic interface circuitry finally performs traditional signal processing functions such as amplification & noise reduction.

8) b) (i) Expression for bending radius of the generated free electrons:

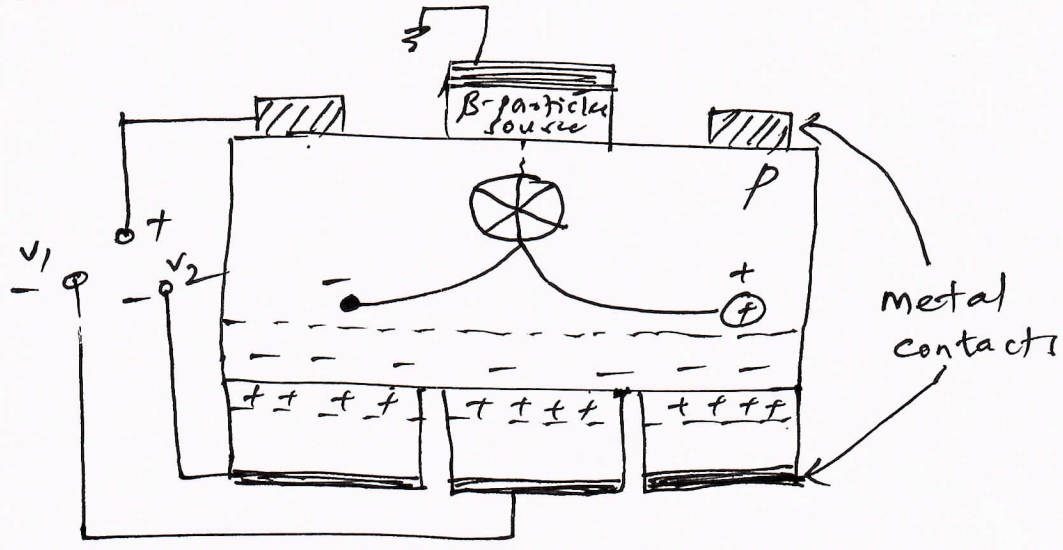

Let us obtain the expressions for the min. initial kinetic energy of the electron, its final kinetic energy and the radius of the arc along its trajectory.

The min. kinetic initial energy is given by:

$$\frac{1}{2} m v_0^2 = \int F \, dl \qquad \text{——— (1)}$$

$$= q \int \vec{E} \cdot dl + q \int (\vec{V} \times \vec{B}) \, dl \qquad \text{——— (2)}$$

where, q → electron's charge
$\vec{E}$ → steady-state electric field
$\vec{B}$ → magnetic flux density
$\vec{V}$ → electrons initial velocity
l → path of integration

Since the magnetic force is always perpendicular to the path,

$$\frac{1}{2} m v_0^2 = q \cdot V \qquad \text{——— (3)}$$

where, V → is the steady-state electrostatic potential or v°. between the terminals of the device.

∴ Min. velocity, $v_0 = \sqrt{\frac{2qV}{m}}$ ——— (4)

$$J = n \cdot q \cdot e_v \qquad \text{——— (5)}$$

Where $J \rightarrow$ current density
$n \rightarrow$ free electron density in p region
$V_e \rightarrow$ terminal velocity of the electron.

$$\therefore nqV_e + pqV_h = 0 \quad \text{——— (6)}$$

Where $p \rightarrow$ hole density
$V_h \rightarrow$ hole's terminal velocity

$$V_e = -\frac{p}{n} V_h \quad \text{——— (7)}$$

$$\therefore V_h = \mu_h \cdot E \quad \text{——— (8)}$$

where $\mu_h \rightarrow$ hole's mobility

Hence, $$V_e = -\frac{p}{n} \cdot \mu_h E$$

$$= -\frac{p}{n} \mu_h \left(\frac{V}{L}\right) \quad \text{——— (9)}$$

$$\therefore \frac{1}{2} m_e v^2 = \frac{1}{2} m v_0^2 e^{-\alpha L} \quad \text{——— (10)}$$

where $\alpha \rightarrow$ attenuation constant

$$\alpha \simeq -\frac{1}{L} \ln\left(\frac{V_e^2}{V_0^2}\right) \quad \text{——— (11)}$$

where V_0 & V_e are the final & the terminal velocities of the electron as previously indicated.

$$\therefore q \cdot V \cdot B = \frac{mV^2}{R} \quad \text{——— (12)}$$

where $R \rightarrow$ radius

$$R = \frac{mV}{qB} = \frac{mV_0}{qB} \cdot \exp\left[\frac{d}{L} \ln\left(\frac{V_e}{V_0}\right)\right] \quad \text{——— (13)}$$

$$\therefore \boxed{R = \frac{mV_e}{qB}}$$

(ii) Derivation of the electron's path in the horizontal direction:

$$x(\theta) = a e^{b\theta} \cos\theta$$
$$y(\theta) = a e^{b\theta} \sin\theta \quad \text{——— (1)}$$

where a & b are constants and θ is a parameter along the curve.

The arc length for any curve is given by

$$l = \int_0^{\theta} \sqrt{[x'(\theta)]^2 + [y'(\theta)]^2} \quad \text{——— (2)}$$

By differentiating $x(\theta)$ & $y(\theta)$

$$l = \frac{a\sqrt{b^2+1}}{b} [\exp(b\theta) - 1] \quad \text{——— (3)}$$

Now θ as a fn of l →

$$\theta = \frac{1}{b} \ln\left[1 + \frac{bl}{a\sqrt{b^2+1}}\right] \quad \text{——— (4)}$$

Since, the exponent 'b' must be a negative number, the max. value of arc length, l_{max} is

$$l_{max} = -\frac{a\sqrt{b^2+1}}{b} \quad \text{——— (5)}$$

substituting eqn (4) & (5) in eqn (1) ⇒

$$x(l) = a\left[1 - \frac{l}{l_{max}}\right] \cos\left(\frac{1}{b} \ln\left[1 - \frac{l}{l_{max}}\right]\right)$$

$$y(l) = a\left[1 - \frac{l}{l_{max}}\right] \sin\left(\frac{1}{b} \ln\left[1 - \frac{l}{l_{max}}\right]\right) \quad \text{——— (6)}$$

Here, $l_{max} = R_0$ then

$$x(l) = a\left[1 - \frac{l}{R_0}\right] \cos\left(\frac{1}{b} \ln\left[1 - \frac{l}{R_0}\right]\right) \quad \text{——— (7)}$$

$$y(l) = a\left[1 - \frac{l}{R_0}\right] \sin\left(\frac{1}{b} \ln\left[1 - \frac{l}{R_0}\right]\right)$$

29

Since $d_{max} = R_0$ then

$$R_0 = \frac{m v_0}{q \cdot B} = - \frac{a\sqrt{b^2+1}}{b} \qquad \text{——— (8)}$$

A second eqn in two unknowns a & b can now be found as:

$$x(l) \simeq x(L) \simeq L \qquad \text{——— (9)}$$

$$\therefore x(L) \simeq L \simeq a\left[1 - \frac{L}{R_0}\right] \cos\left(\frac{1}{b} \ln\left[1 - \frac{L}{R_0}\right]\right) \qquad \text{——— (10)}$$

$$a \simeq L$$

$$\therefore b = \pm \frac{a}{\sqrt{R_0^2 - a^2}} \qquad \text{——— (11)}$$

$$b \simeq -\frac{L}{R_0} \qquad \text{——— (12)}$$

$$\therefore d = R_0\left[1 - \exp\left(b \tan^{-1}\frac{R_0}{L}\right)\right] \qquad \text{——— (12)}$$

9) a) Icing detector.

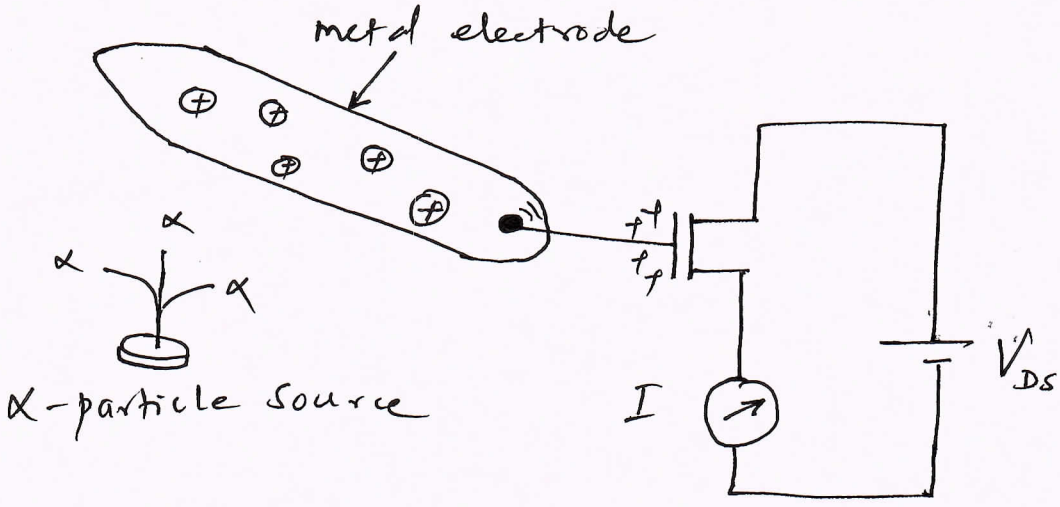

Principle of operation :

Icing detector finds its applications in aircraft. This detector utilizes 'α' particles. An 'α'-particle source is attached to the wing of the aircraft, and a detector that mainly depends on a MOSFET transistor is placed a few centimeters away from the source. As the 'α' particles strike the detector, they deposit their positive charges on the gate of the MOSFET (n-channel), and the transistors turn ON. If, however, a layer of ice builds up on the wings and prevents the α-particles from reaching the detector, the MOSFET shuts OFF.

q) b) **Determination of the turn ON condition of the MOSFET-**

To determine conditions that are necessary for turning ON a MOSFET by means of a flow of positively charged particles.

$$\therefore \quad Q = \int C_{iss}\, dv \qquad \text{——— (1)}$$

$$Q = \int_{V_{DD}-V_{GS}}^{V_{DD}} (C_o + mV)\, dv \qquad \text{——— (2)}$$

where C_o is the initial capacitance at $V_{DS} \neq 0$.

$$V_{GS}^2 - 2V_{GS}\left(V_{DD} + \frac{C_o}{m}\right) + \frac{2Q}{m} = 0 \qquad \text{——— (3)}$$

$$V_{GS} = \left(V_{DD} + \frac{C_o}{m}\right) \pm \sqrt{\left(V_{DD} + \frac{C_o}{m}\right)^2 - \frac{2Q}{m}} \qquad \text{——— (4)}$$

$$J = \sigma E \qquad \text{——— (5)}$$

where $\sigma \rightarrow$ conductivity of SiO_2

$$\therefore \frac{I}{A} = \sigma \frac{V_{GS}}{\Delta x} \qquad \text{——— (6)}$$

$$\therefore V_{GS} = \frac{I \Delta x}{\sigma A} = \left(V_{DD} + \frac{C_o}{m}\right) \pm \sqrt{\left(V_{DD} + \frac{C_o}{m}\right)^2 - \frac{2Q}{m}} \qquad \text{——— (7)}$$

The current $I = \frac{\Delta Q}{\Delta t}$,

$$\therefore V_{GS} = \frac{\Delta Q}{\Delta t}\left(\frac{\Delta x}{\sigma A}\right)$$

$$= \left(V_{DD} + \frac{C_o}{m}\right) \pm \sqrt{\left(V_{DD} + \frac{C_o}{m}\right)^2 - \frac{2\Delta Q}{m}} \qquad \text{——— (8)}$$

Solving for $\Delta Q \Rightarrow$

$$\Delta Q = 2\left(V_{DD} + \frac{C_o}{m}\right)\left(\frac{\sigma A}{\Delta x}\Delta t\right) - \frac{2}{m}\left(\frac{\sigma A}{\Delta x}\Delta t\right)^2$$

Because of very small value of i,

$$\frac{\Delta Q}{\Delta t} = I \simeq 2\left(V_{DD} + \frac{C_0}{m}\right)\frac{\sigma A}{\Delta x} \quad \text{——— (10)}$$

$$C = \epsilon_0 \epsilon_r \frac{A}{\Delta x} \quad \text{——— (11)}$$

$$\frac{\Delta x}{A} = \frac{\epsilon_0 \epsilon_r}{C} \simeq 1.438 \ m^{-1}$$

$$\therefore I = 1.18 \times 10^{-14} \quad A$$

---

10) a) Interface circuit used in icing detector :

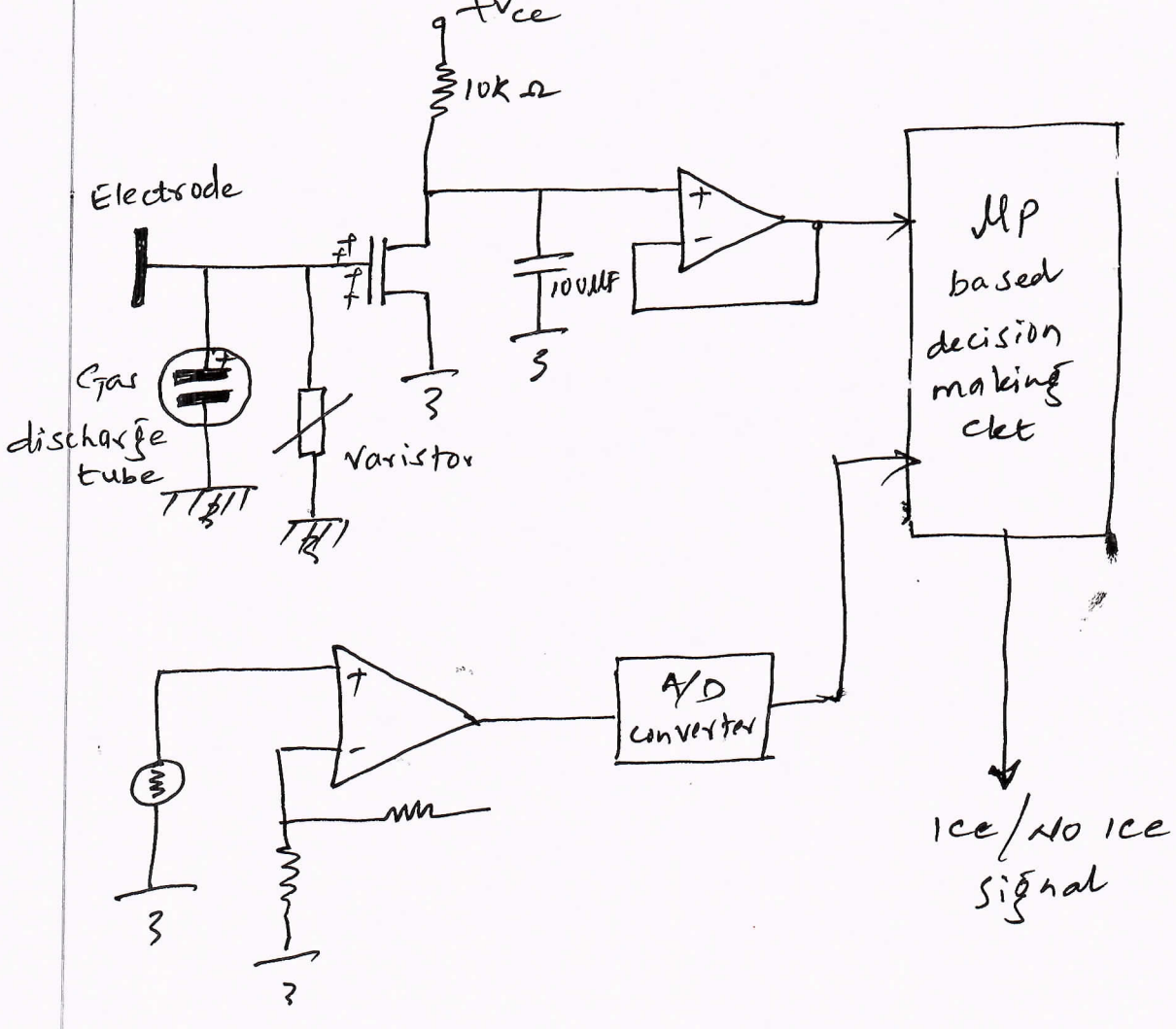

The interface ckt. used is a very basic circuit for sensing the state of the MOSFET. under various operating conditions, and more sophisticated ckts can be used in actual implementations, depending on the type of interface that is desired.

As shown in the ckt, the electrode, which acquires the positive charge, is directly connected to the gate of an n-channel, E-MOSFET. Two surge protection components are also connected to the gate: a gas discharge tube for protection against lightning, and a varistor for dissipating any voltage build-up above 20V. Both components are directly connected to the airframe, as shown, and help to eliminate transients in addition to the main fn of protecting the MOSFET. When the +ve charges are present on the gate of the MOSFET, the device is ON, and hence the o/p vg. is low. If the charge is not present, however, the device is off, and hence the o/p vg. will be high - indicating an alarm. Alarm signal is filtered with a low-pass filter further surpressing the transients. A microprocessor based circuit is used for making a decision about the validity of any alarm signal from the MOSFET.

The presence of ice on the wing is asserted if two conditions are present:

(1) alarm signal from the MOSFET must hold for several seconds; hence any transients are ignored

(2) The thermometer interface ckt must indicate a below-freezing temp. while the alarm signal from the MOSFET is present.

If the above two conditions are satisfied simultaneously, the µp ckt. issues a valid warning signal about the presence of ice on the wing

10) b)

(i) Results of testing with dry ~~air~~, moist air, and super-saturated water vapour -

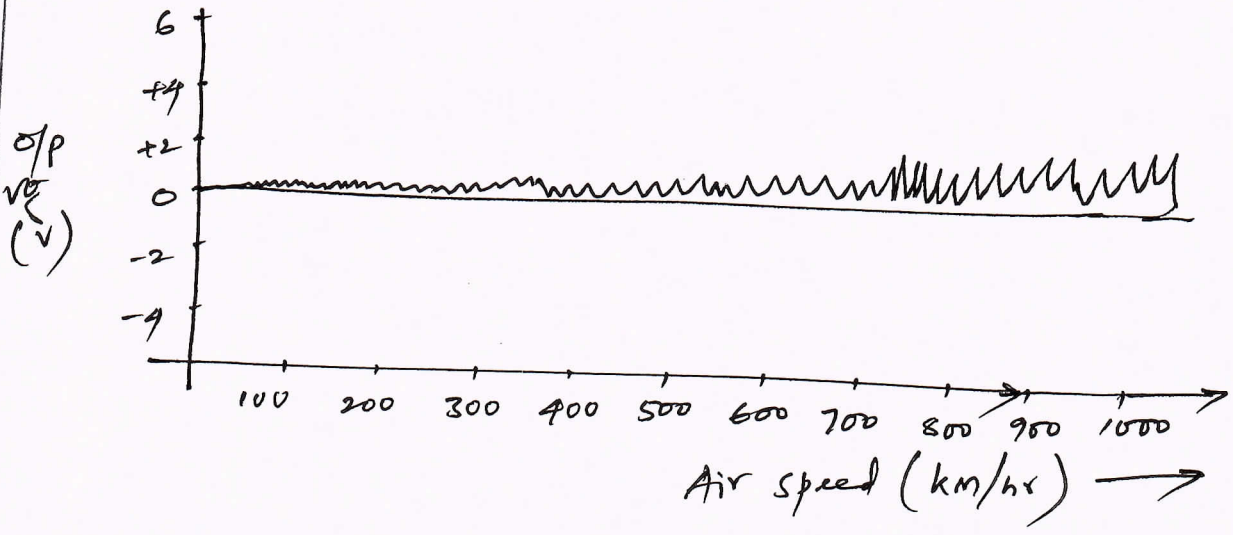

The above graph shows the test results that were conducted with dry air, moist air, & super saturated water vapour. The results are similar for all three conditions.

The figure shows the o/p vg. of the MOSFET, together with the ice/no ice signal provided by the decision making microprocessor circuit. The ice/no ice signal remained at 0V, as shown, while the MOSFET o/p remained generally low.

The slight increase in the o/p vg. of the MOSFET at high air speeds is due to the fact that a very small fraction of the 'α'-particles are swept away from the detector at such speeds.

(ii) Results of testing with small crystal of ice -

This test performed in the winter, while temp. outside the tunnel was below freezing. Natural snow was injected in to the air by using a special pressurized container that was designed by the author's research group. As the snow started accumulating on the

and covering the α-particle source, measurements were taken.

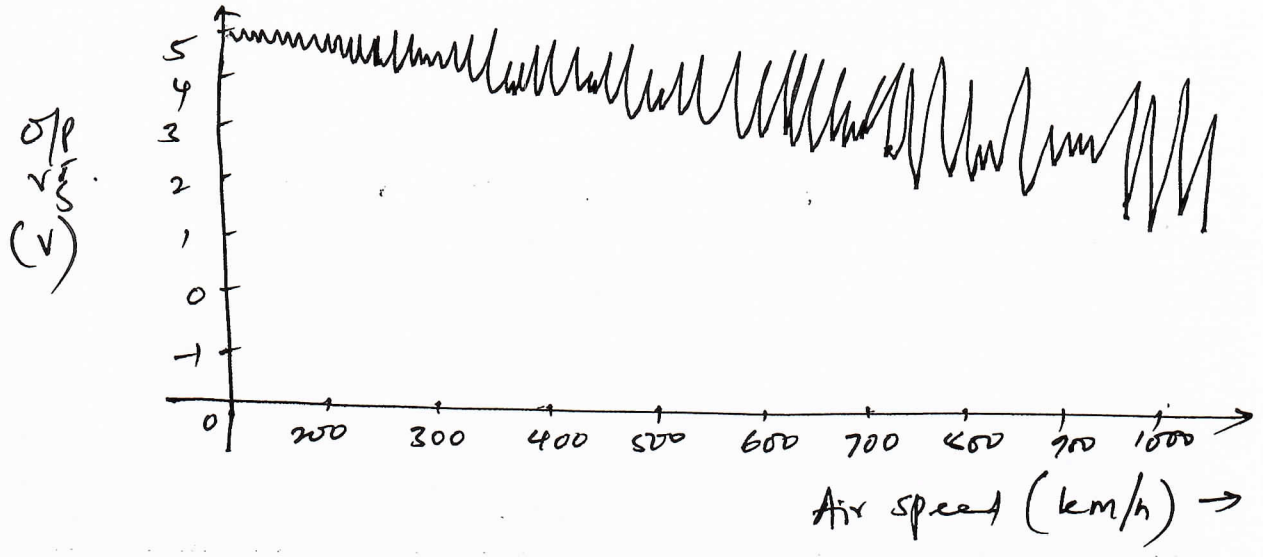

In this case, both the MOSFET o/p & the ice/no ice signals were high, indicating a positive alarm.

(iii) Testing under Lightning strikes -

In this test, lightning was simulated by grounding the air frame and discharging an electrode that was raised to a potential of 2 million volts directly through the detector. As expected, the lightning protection devices included in the detector quickly dissipated the excess charge within a fraction of a second, and although the o/p of the MOSFET swung substantially for a fraction of a second, the transient did not affect the operation of the dectector and no flase alarm was observed.

HEAD
Dept. of Electrical & Electronics Engg.
KLS's V. D. Institute of Technology
HALIYAL-581 329